



Metabolic imaging of *Fragilariopsis cylindrus* in polar night conditions using full-field optical transmission tomography (FFOTT)

NATHALIE JOLI,^{1,5}  CLAUDE BOCCARA,² BENJAMIN BAILLEUL,³
CHRIS BOWLER,¹ AND MARTINE BOCCARA^{1,2,4,*} 

¹*Institut de Biologie de l'École Normale Supérieure (IBENS), École Normale Supérieure, CNRS, INSERM, PSL Université, 75005 Paris, France*

²*Institut Langevin, ESPCI Paris, PSL Research University, CNRS UMR 7587, 1 rue Jussieu, 75005 Paris, France*

³*Laboratory of Chloroplast Biology and Light Sensing in Microalgae, Institut de Biologie Physico Chimique, CNRS, Sorbonne Université, Paris, 75005, France*

⁴*Institut de Systématique, Evolution, Biodiversité (ISYEB), Muséum national d'Histoire naturelle, CNRS, Sorbonne Université, EPHE, Université des Antilles, 57 rue Cuvier, 75005 Paris, France*

⁵*Present address: Institut d'Écologie et des Sciences de l'Environnement de Paris (iEES-Paris), Sorbonne Université, UMR 7618 CNRS-INRA-IRD-Univ. Paris Cité-UPEC, Paris, France*

*martine.boccarda@mnhn.fr

Abstract: FFOTT is a non-invasive, non-destructive method of imaging that was found promising for a broad range of applications. We applied FFOTT to compare intracellular dynamic signals, a proxy for cellular metabolic activity. We investigated the metabolic changes associated with the transition from and towards polar night in the polar diatom *Fragilariopsis cylindrus*, grown under continuous illumination or kept in darkness for six weeks. Our results revealed a tenfold signal decrease in darkness and a rapid signal recovery upon re-illumination. Photosynthetic performance was assessed in parallel. Biovolume determinations allowed the computation of the metabolic rates of *F. cylindrus* grown under both light and dark conditions, which were compared to the optical signal variations.

© 2026 Optica Publishing Group under the terms of the [Optica Open Access Publishing Agreement](#)

1. Introduction

Label-free microscopy methods are valuable to investigate biological systems without disrupting their physiology or integrity. Full Field Optical Transmission Tomography (FFOTT) is a label-free, non-destructive imaging technique based on the use of π phase shift first observed by Gouy [1]. Specifically, a phase shift occurs between the transmitted illumination beam and the light scattered by sub-micron structures, depending on their position relative to the microscope objective focus. By exploiting the interference between the illumination beam and the scattered one, FFOTT generates tomographic images of cellular structures by subtracting two images acquired at planes separated by half the depth of field. When operated in dynamic mode, it provides a functional contrast sensitive to intracellular movement and metabolic activity as already observed in Full field optical coherence tomography (FFOCT) [2,3]. To develop FFOTT applications, we used a basic home-made set up or a cheap commercial microscope [4].

We previously demonstrated that FFOTT can detect stress-related metabolic changes in the diatom *Phaeodactylum tricornutum* [5]. Under photosystem II inhibition, the dynamic signal sharply decreased and a similar decrease was observed with non-photosynthetic-dependent illumination [5]. These experimental results further support the interpretation of the FFOTT dynamic signal as a proxy for metabolic activity. The method has also been applied in other systems, from cancer cells to environmental samples [6,7], illustrating its broad relevance from medical to biological applications.

Here, we apply FFOTT to the polar diatom *Fragilariopsis cylindrus*, a model organism particularly well-suited for studying hypometabolism, the reduction of cellular activity in response to light conditions. In a previous study [8], we demonstrated that *F. cylindrus* survives simulated polar night condition by entering a quiescent state, characterized by a strong reduction in metabolic activity and a halt in cell division. This remarkable resilience enables polar diatoms to withstand extended darkness and quickly resume photosynthesis and growth when light returns; an ecologically crucial trait, as diatoms dominate polar phytoplankton blooms and underpin marine food webs. Building on these findings, we used FFOTT to compare the dynamics of *F. cylindrus* cells acclimated to continuous light with those exposed to darkness for durations ranging from 16 hours (h) to six weeks (6w), with six weeks corresponding to a period previously shown to induce a stable hypometabolic state. We also examined the response upon re-exposure to light after 2 h and 24 h of recovery, the latter duration being sufficient to fully restore cellular activity. Our results revealed a tenfold decrease in signal during darkness and a rapid recovery upon re-illumination, validating FFOTT as a non-invasive method for monitoring metabolic states in living cells.

We also assessed photosynthetic performance across the same conditions. In agreement with previous work [8], photosynthetic capacity was found to be largely preserved during extended darkness and quickly restored upon light return.

Numerous studies have shown the relationships between microorganism size and physiological or anatomical traits also known as allometric scaling [9,10]. Allometric scaling establishes by a power law the relationship between the size (volume) and the metabolic rate of various organisms. Metabolic rate can be expressed as the ATP_{eq} (adenosine triphosphate equivalent) requirements for growth. Based on this relationship we computed the energy needed by *F. cylindrus* to survive in the dark for long time period and attempted to relate it to the optical signal we measured.

2. Material and methods

2.1. Preparation of *Fragilariopsis* samples

Triplicate axenic batch cultures of *F. cylindrus* CCMP3323 were maintained in Aquil medium [11], at 4 °C under a continuous low white light level (30 μmol photons m⁻² s⁻¹) in 300 mL flasks without agitation. To simulate polar night conditions, exponentially growing, light-acclimated cultures (10⁶ cells mL⁻¹) were transferred to complete darkness for up to six weeks by wrapping the flasks in aluminum foil. After dark incubation, cultures were returned to the original light conditions. Samples were collected at the following time points: during light acclimation (T0L), after 16 h in darkness (D16 h), after 6 weeks (D6w) in darkness, and after 2 h (RL2 h) and 24 h (RL24 h) following re-exposure to light as illustrated in Fig. 1. Cells from dark-grown samples were collected under red light to avoid light-induced responses. Cellular concentrations were measured from culture aliquots using a flow cytometer CyFlow Cube 8 (Sysmex).

For FFOTT analysis, cells were harvested by centrifugation and embedded in molten 1% agar (42 °C) prepared in Aquil medium. For samples of dark-grown cells, all manipulations and imaging were conducted under dim red light. Samples were imaged immediately after gel solidification at room temperature (20 °C). When required, Photosystem II activity was inhibited by incubating cultures with 40 μM of 3-(3,4-dichlorophenyl)-1,1-dimethylurea (DCMU), dissolved in ethanol, for 10 minutes at room temperature prior to embedding.

2.2. Photosynthetic measurements

The ratio Fv/Fm which indicates the maximum yield of PSII (Photosystem II) was determined as described in detail in [8], after few minutes in darkness. The effective absorption cross section for Photosystem II (σPSII) was determined from the chlorophyll fluorescence induction curve provoked by a single turnover flash or train of repeated flashlets [12], applied in dark-acclimated



Fig. 1. Sampling time points during light–dark–light transition in *Fragilariopsis cylindrus*. Cultures were sampled during the acclimation phase under continuous low light (TOL), then transferred to complete darkness for up to six weeks. Additional samples were collected after 16 h in darkness (D16 h) and at the end of the dark period of six weeks (D6w). Upon re-exposure to light, samples were taken after 2 h (RL2 h) and 24 h (RL24 h) of recovery. The light/dark transitions are represented as a horizontal timeline (yellow: light, grey: darkness).

cells. The PSII yield (φ PSII) was measured after at least 4 minutes of blue light (450 nm) illumination (I) at $24 \mu\text{mol photons}\cdot\text{m}^{-2}\cdot\text{s}^{-1}$ and used to calculate the electron transfer rate (ETR) under this illumination as in [8] : $\text{ETR} = \sigma\text{PSII} * \varphi\text{PSII} * I$.

2.3. Data acquisition and analysis

To monitor the intracellular dynamics of scattering structures, we analyzed the temporal variation of optical tomographic signals at the pixel level across image stacks. The Full Field Optical Transmission Tomography (FFOTT) method is described in detail in [3]. Briefly, the sample is illuminated in transmission with incoherent light from LEDs (455 nm and 617 nm in this study). Light transmitted through and light scattered by the sample interfere, the Gouy phase that takes place very close to focus is the dominant phase shift close to the microscope objective focus. Indeed, the Gouy phase shift depends on the relative position of the scatterers and the objective focus. These interference patterns are recorded over time using a Photonfocus A1024B CMOS camera.

Typically, stacks of 100 images were acquired at 138 Hz from at least three fields of view, each stack was imaged at three distinct focal depths. Image sequences were analyzed using Fiji [13], including visualization of transmission images to assess cell stability, static tomographic reconstructions to identify intracellular structures (differences between two z-stack sections separated by 500 nm in depth), and the standard deviation projection to reveal dynamic signals. The dynamic signal was visualized using ImageJ (16-color scale) [5], or Matlab. We computed the entire signal of the standard deviation image (number of cells about 10) and subtracted the background signal (cellfree regions) to determine the dynamic signal. Box plot analysis represents the signal from 24 to 40 stacks corresponding to about 300 cells (at least, 3 repeats of each condition, 3 fields per repeat, 3 stacks at different depths per field).

All statistical analyses of distribution were performed with the Wilcoxon test (significance level $P < 0.001$ or $P < 0.005$).

3. Results and discussion

3.1. Reversible reduction of metabolic activity in darkness inferred from FFOTT imaging

Using our setup and illumination with a 455 nm LED, known to be efficiently absorbed by *F. cylindrus*, being close to the maximum absorption, we measured the dynamic signal in cells acclimated to full light condition. Two key sites of dynamic signal changes were identified: vesicles and the chloroplast membrane (Fig. 2(A)). The vesicles, likely lipid droplets (LD), of different sizes, have previously been confirmed by staining with BODIPY [8].

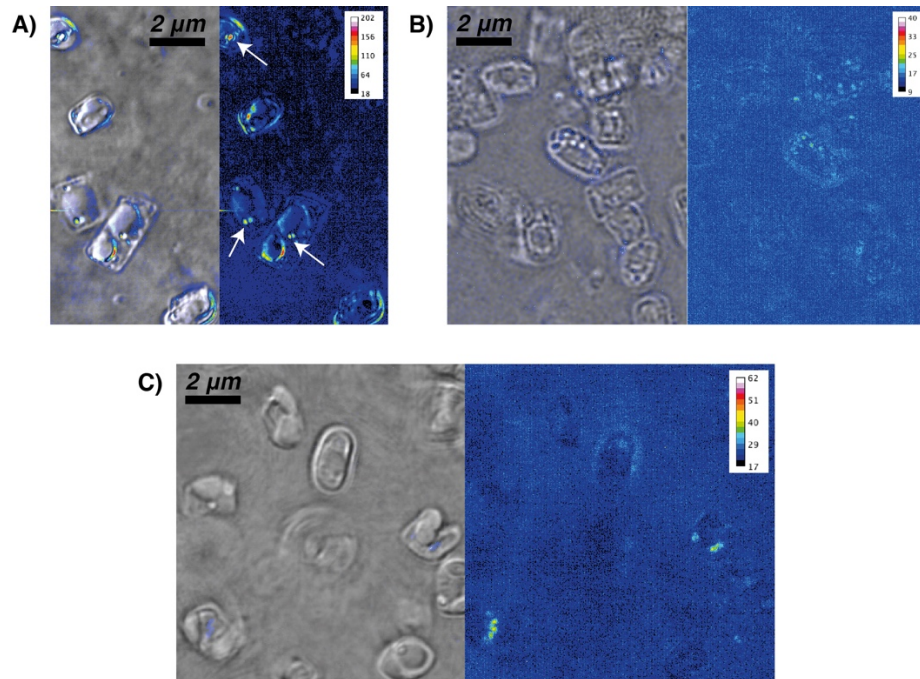


Fig. 2. FFOTT dynamic signal in *F. cylindrus* cells grown under full light versus prolonged darkness. Dynamic signal was recorded in cells acclimated to continuous light (T0L) and in cells exposed to six weeks of complete darkness (D6w). For each panel, the left image shows the difference between two optical sections spaced by 500 nm in depth, overlaid with the corresponding standard deviation (STD); the right image shows the STD projection of the full z-stack, with the intensity scale indicating that red corresponds to the highest signal amplitude and dark blue represents the lowest signal and background. **A)** Cells at T0L imaged with a 455 nm LED. Arrows indicate dynamic signal in lipid droplets. **B)** Cells at T0L imaged with a 617 nm LED. **C)** Cells at D6w imaged with a 455 nm LED.

In cells illuminated with orange light (LED, 617 nm), the dynamic signal inferred from imaging was markedly reduced (Fig. 2(B)). The wavelength of 617 nm LED corresponds to a spectral region close to a minimum of absorption by photosynthetic pigments in *F. cylindrus* and diatoms in general and where photosynthesis is at a minimum. A similarly low signal was detected in cells treated with DCMU, a photosystem II inhibitor (Fig S1). Together, these results strongly indicate that the signal depends on photosynthetic activity and reflects the metabolic activity of the cells strictly dependent on photosynthesis.

This signal was drastically reduced, by approximately tenfold after six weeks of complete darkness (Fig. 2(C)), reaching levels comparable to those observed under 617 nm illumination or in the presence of DCMU for light condition (Fig. 3, S1). Notably, the decline in signal was already evident after only 16 h of darkness (Fig. 4(A)), suggesting that the response is both rapid and tightly linked to light availability.

To determine whether the signal could recover after prolonged darkness, we re-illuminated cells kept in darkness for six weeks for either 2 h or 24 h. After 2 h, the signal remained indistinguishable from that of fully dark-acclimated cells (Fig. 4(A)). However, after 24 h of re-exposure to light, the signal partially recovered, reaching approximately half the intensity observed in cells maintained in continuous light (Fig. 4(A), 4(B)). These observations confirm that the signal captured by FFOTT is both dynamic and reversible, and suggest that metabolic

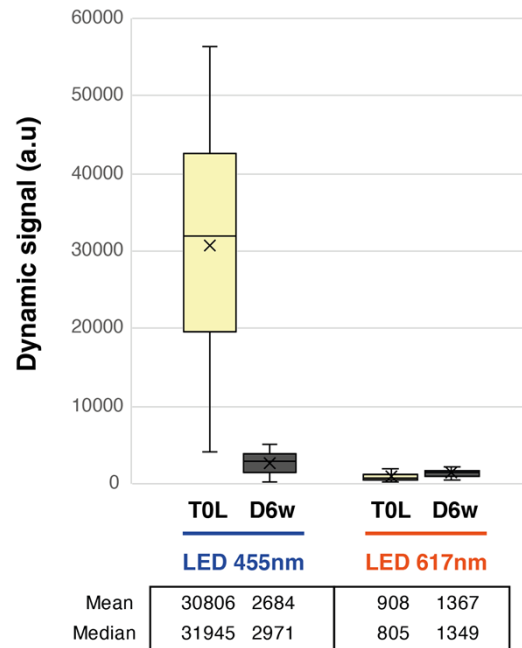


Fig. 3. Prolonged darkness reduces the dynamic signal of *F. cylindrus*. Box plot of dynamic metabolic signal (arbitrary units, a.u.) in cells acclimated to continuous light (TOL) versus cells exposed to six weeks of darkness (D6w). Measurements were performed using LED 455 nm (blue) or 617 nm (orange). Signal above background was quantified using ImageJ from 20–40 time-lapse sequences per condition. Solid line and cross indicate the median and the mean respectively, the whiskers extend to the minimum and maximum values.

activity probed by FFOTT is reactivated only 24 h upon return to light. This dynamic response is consistent with the remarkable resilience of *F. cylindrus* previously described during recovery from extended periods of darkness [8].

The integrity and functionality of PSII was preserved even after extended periods in darkness as assessed by the stability of Fv/Fm throughout the experiment, around 0.4 (Fig. 5(A)). A slight decrease in σ PSII suggests a modest reduction in light-harvesting capacity upon prolonged darkness, yet the overall potential for PSII photochemistry remained comparable in light acclimated and dark acclimated cells (Fig. 5(B)). To investigate the capacity for PSII electron transfer rate in the two conditions, we calculated ETR under $24 \mu\text{mol photons}\cdot\text{m}^{-2}\cdot\text{s}^{-1}$ of blue actinic light, comparable to the wavelength used for FFOTT (see Methods). This intensity was chosen to reach comparable light absorption as in growth conditions ($30 \mu\text{mol photons}\cdot\text{m}^{-2}\cdot\text{s}^{-1}$ of white light). ETR strongly declined after six weeks of darkness, reflecting a temporary loss of photosynthetic capacity. However, it rapidly recovered within 2 h of light exposure and returned to light-acclimated levels after 24 h, demonstrating the reversible nature of this decline (Fig. 5(C)). While these measurements reflect the photosynthetic activity in light, they only inform about the photosynthetic capacity for cells acclimated to darkness. These data confirm that photosynthetic activity itself resumed partially within 2 h of light return and completely after one day, consistent with previous observations [8].

Interestingly, this pattern diverges from that observed in the dynamic FFOTT signal, which requires 24 h to fully recover but is null after 2 h. These findings indicate that photosynthesis is necessary for detecting a dynamic signal by FFOTT, given its sensitivity to DCMU inhibition, but not sufficient, as a temporal delay exists between the restoration of photosynthetic activity

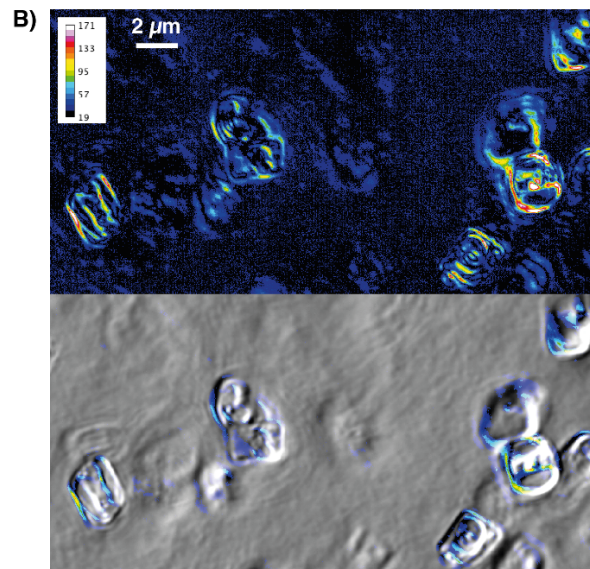
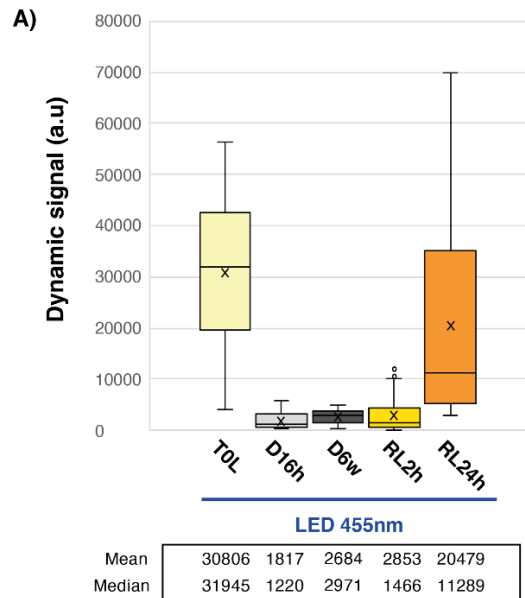


Fig. 4. Dynamic signal is reduced in darkness and restored after 24 h of light exposure.

A) Dynamic signal measured in cells grown in continuous light (TOL), then kept in darkness for 16 h (D16 h) or six weeks (D6w), or re-exposed to light for 2 (RL2 h) or 24 h (RL24 h) after six weeks in darkness. Cells were illuminated with a 455 nm LED, and the dynamic signal above background was quantified. For each condition, 20–40 movies of 100 images were analyzed using ImageJ. Solid line and cross indicate the median and the mean respectively, the box represents the interquartile range (25th–75th percentile), and whiskers extend to the minimum and maximum values. . . **B)** Dynamic signal in cells re-exposed to light for 24 hours after two months in darkness. **Top:** standard deviation (STD) of all images in a stack (LED 455 nm). **Bottom:** difference between two images separated by 500 nm in depth, merged with the STD.

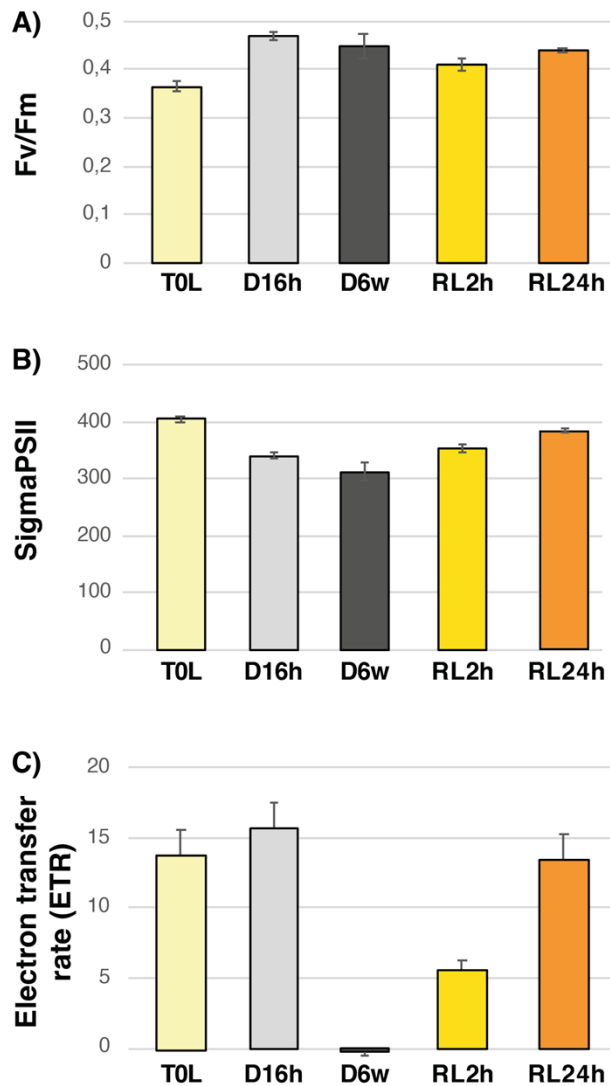


Fig. 5. : Photosynthetic potential is preserved during prolonged darkness and restored upon return to light. **A)** Maximum quantum efficiency of photosystem II (Fv/Fm). **B)** Average effective absorption cross-section of PSII (σ_{PSII} , in \AA^2), measured using a mini FIRE (Fluorescence Induction and Relaxation) system. **C)** Maximum relative electron transport rate (rETRmax, in $\mu\text{mol photons m}^{-2} \text{s}^{-1}$).

and the recovery of intracellular dynamics measured by FFOTT, at the individual cell level. This difference suggests that the FFOTT signal does not capture photosynthetic activity but metabolic activity downstream photosynthesis, such as the export of photosynthates or lipids across the chloroplast membranes, or the transport of other molecules which slowly accumulate after light return.

3.2. Metabolic signification of the dynamic signal

Cells maintained in darkness for six weeks exhibited a significantly reduced number of lipid droplets (LD) compared to cells maintained in continuous light or after 16 h of darkness (Fig. 6).

This reduction is partially reversed after 24 h of light re-exposure, with an increased number of LD, although not fully restored to initial levels. These results suggest that extended darkness depletes lipid stores, which begin to be replenished upon return to light. This pattern is consistent with our previous BODIPY staining in similar light–dark–light experiments, where cells mobilized lipid reserves during extended darkness to maintain basal activity, and replenished them upon one day of re-illumination [8].

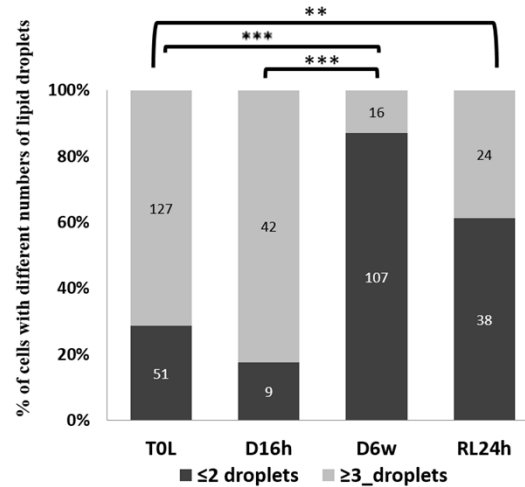


Fig. 6. Histogram of the number of lipid droplets in cells in different culture conditions.

Cells were grown either in light or kept in darkness for 16 hours (D16 h) or 6 weeks (D6w) and cells returning to light for 24 hours after six weeks of darkness (RL24). Cells were classified into two groups: cells with at least two droplets (dark grey) or cells with three or more droplets (light grey). The numbers indicate the number of cells considered for droplet counting. A Wilcoxon statistical test was performed: *** $P < 0.001$; ** $p < 0.005$ (Table S1).

The dynamic signal in light-grown cells is primarily localized to LD (Fig. 2(A)). However, the presence of LD alone does not predict their dynamic behavior: after 16 h of darkness, LDs remain abundant (Fig. 6, image S1) but show no detectable dynamics in FFOTT (Fig. 4(A)). In contrast, cells re-illuminated for 24 h after six weeks of darkness exhibit both an intermediate number of LD and a partially restored dynamic signal (Fig. 4(B)), suggesting that signal recovery parallels LD replenishment.

To explore whether FFOTT dynamics in LD reflects lipid metabolic activity, such as triacylglycerol (TAG) fluxes, we computed the FFOTT signal using two metrics: the standard deviation (STD), quantifying signal amplitude, and the cumulative sum (CumSum), which captures biased random movement of intracellular scatterers [14]. A significantly higher CumSum/STD ratio was observed in light-exposed cells (6 ± 0.35) compared to dark-adapted cells (3.7 ± 0.18), close to the background value (3.4) (Image S2). These results support the idea that dynamic fluctuations in LD are more pronounced under light conditions and may reflect intracellular trafficking of TAG, synthesized in chloroplasts and stored in endoplasmic reticulum-derived vesicles surrounding the chloroplast [15].

These findings provide insight into the interplay between lipid metabolism and light exposure, showing that the dynamic signal in LD is linked to changes in TAG storage and mobilization, both of which appear to be influenced by light conditions.

3.3. Insights into metabolic allometric scaling

Lynch and Marinov [16], computed the total energetic requirements of a unicellular microorganism for growth (C_T), as the number of ATP hydrolysis events during cell growth (C_G) plus the number of ATP molecules necessary for maintenance (C_M or basal energy/h). There is an allometric scaling relationship between metabolic activity of unicellular organisms and cell volume, which can be written: $C_T = C_G + t C_M$ with $C_G = 26.92 V^{0.32}$ and $C_M = 0.39 V^{0.29}$ and where V is the cell volume, t the generation time (36 h for growth conditions of *F. cylindrus*) and the exponent function of growth temperature (see [Supplement 1 S1](#) for detail calculation). To compute the volume of *F. cylindrus* grown at light at 4°C, we assimilated the shape of *F. cylindrus* to a prolate ellipsoid [17] and determined an average volume V of $30 \pm 11 \mu\text{m}^3$ (fig S2, Table S2). We computed the average total energy of cell grown at 4°C with light as $8.07 \cdot 10^{10}$ ATP_{eq} per cell.

When cells are kept in darkness, they are in a quiescent state which cannot be referred to the basal energetic metabolism (see [16]). We thus used published metabolic indicators such as oxygen consumption and carbon fixation to consider a ten times reduction in cellular metabolism when cells were kept at dark for six weeks [18,8].

We hypothesized that *F. cylindrus* uses energy mostly from LD for its survival in darkness. We estimated the number of TAG (triacylglycerol) molecules per lipid droplet to deduce the number of ATP currency provided by the consumption of one LD in darkness. The degradation of the TAGs of one lipid droplet would generate theoretically $3\text{--}12 \cdot 10^9$ ATP equivalents (see [Supplement 1 S1](#) for detail calculation). We thus propose that the consumption of $8 \cdot 10^9$ ATP molecules per cell corresponds to the energy of about 3 small (radius = 0.15 μm) or 1 large LD (radius = 0.25 μm) during the six weeks of darkness.

4. Conclusions

Using a simple and accessible optical method based on dynamic imaging, we quantitatively assessed the metabolic activity of *F. cylindrus* under prolonged darkness and re-illumination. The signal, tenfold stronger in light-grown cells than in those kept in darkness for six weeks, correlates with known reductions in overall metabolic activity and ATP content [8,19]. Its sensitivity to photosynthetic inhibition (with DCMU) or to light quality (617 vs 455 nm) confirms its physiological relevance and links it directly to photosynthetic function.

Our analysis also revealed that, although the photochemical potential (Fv/Fm) and absorption cross-section of PSII remains stable, the recovery of intracellular dynamics lags behind the reactivation of photosynthetic capacity. Lipid droplets, often near the chloroplast, emerge as central metabolic players: they become less dynamic and fewer in number during darkness. The CumSum/STD ratio further supports the hypothesis that the dynamic signal reflects fluxes, potentially lipid accumulation rather than consumption.

Altogether, this approach provides a sensitive, quantitative readout of cell metabolism at the single-cell level, offering promising applications for studying energy management and metabolic resilience in microalgae, especially in the context of environmental fluctuations and climate change [20]. The method could also be advantageously applied to cancer cells therapy as already described using FFOCT [21].

Funding. HFSP project Green Life in the Dark (grant RGP0003/2016); European Research Council (Diatomic; grant agreement no. 835067).

Acknowledgment. We acknowledge the Langevin OCT and CB groups for support and encouragement. We warmly thank Pavla Debeljak for proofreading.

Disclosures. The authors declare no conflicts of interest.

Data availability. Data (stacks) underlying the results presented in this paper are not publicly available at this time but may be obtained from the authors upon request.

Supplemental document. See [Supplement 1](#) for supporting content.

References

1. L. G. Gouy, "Sur une propriété nouvelle des ondes lumineuses," *C. R. Acad. Sci. Paris* **110**, 1251 (1890).
2. T. Monfort, S. Azzollini, J. Brogard, *et al.*, "Dynamic full-field optical coherence tomography module adapted to commercial microscopes allows longitudinal in vitro cell culture study," *Commun. Biol.* **6**(1), 992 (2023).
3. V. Mazlin, O. Thouvenin, S. Alhaddad, *et al.*, "Label free optical transmission tomography for biosystems: intracellular structures and dynamics," *Biomed. Opt. Express* **13**(8), 4190–4203 (2022).
4. C. Boccara, V. Mazlin, O. Thouvenin, *et al.*, (2023) *Static and Dynamic Full Field Optical Transmission Tomography in the 100/500 \$ range*; in *PHOTONICS_WEST_CONFERENCES: Optics and Biophotonics in Low-Resource Settings*.
5. H. Bey, F. Charton, H. Cruz de Carvalho, *et al.*, "Dynamic Cell Imaging: application to the diatom *Phaeodactylum tricorutum* under environmental stresses," *European Journal of Phycology* **58**(2), 145–155 (2023).
6. E. Teston, M. Sautour, L. Boulnois, *et al.*, "Label-free optical transmission tomography for direct mycological examination and monitoring of intracellular dynamics," *J. Fungi. (Basel)* **10**(11), 741 (2024).
7. S. Alhaddad, O. Thouvenin, M. Boccara, *et al.*, "Comparative analysis of full-field OCT and optical transmission tomography," *Biomed. Opt. Express* **14**(9), 4845–4861 (2023).
8. N. Joli, L. Concia, K. Mocaer, *et al.*, "Hypometabolism to survive the long polar night and subsequent successful return to light in the diatom *Fragilariopsis cylindrus*," *New Phytol.* **241**(5), 2193–2208 (2024).
9. A. J. Spence, "Scaling in biology," *Curr. Biol.* **19**(2), R57–R61 (2009).
10. J. P. DeLong, J. G. Okie, M. E. Moses, *et al.*, "Shifts in metabolic scaling, production, and efficiency across major evolutionary transitions of life," *Proc. Natl. Acad. Sci. U.S.A.* **107**(29), 12941–12945 (2010).
11. F. M. M. Morel, J. G. Rueter, D. M. Anderson, *et al.* (1979) Aquil: a chemically defined phytoplankton culture medium for trace metals studies. *J. Phycol.* **15**(2): 135–141
12. Z. S. Kolber, O. Prášil, and P. G. Falkowski, "Measurements of variable chlorophyll fluorescence using fast repetition rate techniques: defining methodology and experimental protocols," *Biochimica et Biophysica Acta (BBA) - Bioenergetics* **1367**(1-3), 88–106 (1998).
13. J. Schindelin, I. Arganda-Carreras, E. Frise, *et al.*, "Fiji: an open-source platform for biological-image analysis," *Nat. Methods* **9**(7), 676–682 (2012).
14. J. Scholler, "Motion artifact removal and signal enhancement to achieve in vivo dynamic full field OCT," *Opt. Express* **27**(14), 19562–19572 (2019).
15. A. Jaussaud, J. Lupette, J. Salvaing, *et al.*, "Stepwise biogenesis of subpopulations of lipid droplets in nitrogen starved *Phaeodactylum tricorutum* cells," *Front. Plant Sci.* **11**, 48 (2020).
16. M. Lynch and K. MarinovG (2015) The bioenergetic costs of a gene, PNAS, 112 15690–15695
17. J. Sun and D. Liu, "Geometric models for calculating cell biovolume and surface area for phytoplankton," *J. Plankton Res.* **25**(11), 1331–1346 (2003).
18. P. I. Morin, T. Lacour, P. L. Grondin, *et al.*, "Response of the sea-ice diatom *Fragilariopsis cylindrus* to simulated polar night darkness and return to light," *Limnol. Oceanogr.* **65**(5), 1041–1060 (2020).
19. F. Kennedy, A. Martin, J. P. Bowman, *et al.*, "Dark metabolism: a molecular insight into how the Antarctic sea-ice diatom *Fragilariopsis cylindrus* survives long-term darkness," *New Phytol.* **223**(2), 675–691 (2019).
20. A. Clarke and K. P. P. Fraser, "Why does metabolism scale with temperature?" *Functional Ecology* **18**(2), 243–251 (2004).
21. S. Park, T. Nguyen, E. Benoit, *et al.*, "Quantitative evaluation of the dynamic activity of HeLa cells in different viability states using dynamic full-field optical coherence microscopy," *Biomed. Opt. Express* **12**(10), 6431–6441 (2021).